Optical Materials 143 (2023) 114273

Contents lists available at ScienceDirect

Optical Materials

journal homepage: www.elsevier.com/locate/optmat

Research Article

Optical properties of $Zn_{0.75}Mg_{0.25}O$:Mn ceramics

I. Markevich [a], N. Korsunska [a], T. Stara [a], Yu. Polishchuk [a], I. Vorona [a], K. Kozoriz [a], S. Ponomaryov [a], O. Melnichuk [b], L. Melnichuk [b], A. Cremades [c], L. Khomenkova [a,d,*]

[a] V. Lashkaryov Institute of Semiconductor Physics of National Academy of Sciences of Ukraine, 45, Pr. Nauky, Kyiv, 03028, Ukraine
[b] Mykola Gogol State University of Nizhyn, 2 Hrafska Str., Nizhyn, 16600, Ukraine
[c] Dept. Física de Materiales, Facultad de Físicas, Universidad Complutense de Madrid, 28040, Madrid, Spain
[d] National University "Kyiv-Mohyla Academy", 2 Skovorody str., 04070, Kyiv, Ukraine

ARTICLE INFO

Keywords:
Ceramics
Oxides
Luminescence
X-ray diffraction
Electron spin resonance

ABSTRACT

Mn-doped ZnO, MgO and $Zn_{0.75}Mg_{0.25}O$ samples ([Mn] = 0.1 at.%) were produced by conventional solid-state technique and investigated by means of XRD, EPR, absorption, photocurrent, photo- and cathodoluminescence methods. It was shown that $Zn_{0.75}Mg_{0.25}O$ solid solution with hexagonal structure has the bandgap of E_g ~3.65 eV. The quenching of host defect-related luminescence in ZnO:Mn and in hexagonal $Zn_{0.75}Mg_{0.25}O$:Mn was observed, while the Mn-related emission being absent. The energy level of Mn_{Zn}^{2+} center in hexagonal $Zn_{0.75}Mg_{0.25}O$:Mn was found to be at 2.16 eV below conduction band (*c*-band) bottom and all excited states of Mn_{Zn}^{2+} ions, including the lowest one, reside in *c*-band, as it takes place in ZnO:Mn. It is concluded that the necessary condition to obtain Mn-related light emission in Mn-doped alloys is to make deeper the lowest excited level of Mn_{Zn}^{2+} ions. One of the solutions is to produce $Zn_{1-x}Mg_xO$:Mn solid solution with the bandgap energy larger than 4.0 eV using nonequilibrium fabrication approaches.

1. Introduction

Wide-bandgap semiconductors doped with transition metal ions, in particular, with manganese are promising materials for luminophores in which the emission can be excited both by UV light and high electric field. In the latter case, free electrons accelerated by an electric field impact some of their energy to excite substitutional transition metal ions which then relax radiatively back to their ground state. Mn-related emission has been observed in many wide-bandgap II-VI compounds. Doped with manganese ZnS, ZnSe and CdS materials are known to demonstrate bright photo- and electroluminescence in 590-560 nm (2.1–2.2 eV) spectral range. This emission was shown to originate from intra-shell $^4T_1 - {}^6A_1$ transitions in photo- or electro-excited Mn^{2+} centers [1–4]. However, no such emission was observed in Mn-doped ZnO.

Zinc oxide, a II-VI semiconductor with direct bandgap energy of E_g~3.3 eV at room temperature, is considered as a promising material for versatile device fabrication due to its low cost, high chemical stability, non-toxicity and high radiation resistance. This compound attracts much attention due to its possible application for blue/UV-lasers, light-emitting diodes and photodetectors. Large exciton binding energy (60 meV) allows obtaining bright UV emission and optical lasing at room temperature. In addition, ZnO demonstrates visible emission which spectrum and intensity can be controlled by certain treatments as well as by doping with different impurities.

One of the extensively investigated impurities in zinc oxide is manganese because of ZnO:Mn is considered as a potential high-temperature ferromagnetic. At the same time, manganese dopant in zinc oxide acts as a luminescence "killer" and results in the quenching of both excitonic and defect-related visible luminescence [4–8], but, in contrast to ZnS:Mn and ZnSe:Mn, this quenching is not accompanied by appearance of Mn-related emission [4,5,7,8]. Meanwhile, EPR and absorption spectra studies testify that Mn_{Zn}^{2+} centers are formed in ZnO under manganese doping [9,10] and photoionization of these centers, namely $Mn_{Zn}^{2+} \rightarrow Mn_{Zn}^{3+}$ transitions take place, which gives rise to the formation of a broad unstructured absorption band arising below the onset of band-to-band transitions as well as to the appearance of photoconductivity in the same spectral region, i.e. 400–620 nm (3.0-2.0 eV) [7,8,10–12]. The production of free electrons due to the photoionization of Mn_{Zn}^{2+} centers indicates that all excited states of these centers reside in the *c*-band, which results in the nonradiative relaxation of Mn_{Zn}^{3+} ions back to the ground state [8].

A similar situation is observed in bulk CdSe:Mn as well as in CdSe:Mn

* Corresponding author. V. Lashkaryov Institute of Semiconductor Physics of National Academy of Sciences of Ukraine, 45, Pr. Nauky, Kyiv, 03028, Ukraine.
E-mail addresses: khomen@isp.kiev.ua, l.khomenkova@ukma.edu.ua (L. Khomenkova).

https://doi.org/10.1016/j.optmat.2023.114273
Received 3 May 2023; Received in revised form 21 July 2023; Accepted 18 August 2023
Available online 30 August 2023

quantum dots (QDs) with particle size d > 3.3 nm, in which exited states of Mn_{Cd}^{2+} ions reside in the *c*-band [7]. Doping of this material with manganese caused the quenching of excitonic luminescence, while Mn-related emission was absent. At the same time, the photoluminescence (PL) band caused by Mn_{Cd} $^4T_1 \rightarrow {}^6A_1$ transitions appears in CdSe:Mn quantum dots with a diameter of 3.3–2.5 nm, when band-gap value E_g becomes larger than the energy of $Mn_{Cd}^{2+} \rightarrow Mn_{Cd}^{3+}$ transition and Mn_{Cd}^{2+} ion excited states put down to the band gap. This PL band is observed at about 570 nm (2.18 eV), its position being independent of dot size [7].

In ZnO:Mn quantum dots, however, Mn-related emission has not been observed, which can be accounted for by insufficient enlargement of band gap ΔE_g [7,13].

It is known that the bandgap of ZnO-based materials can be essentially extended by alloying zinc oxide with magnesium oxide. One might expect that Mn-related emission caused by $^4T_1 \rightarrow {}^6A_1$ transitions in Mn_{Zn}^{2+} ions could be obtained in $Zn_{1-x}Mg_xO$ alloys with hexagonal structure. To verify this assumption, in the present work hexagonal-structure $Zn_{1-x}Mg_xO$:Mn ceramics were prepared and their optical characteristics were investigated.

2. Experimental details

Ceramic samples of $Zn_{1-x}Mg_xO$:Mn ($x = 0$, $x = 0.25$ and $x = 1$) were prepared by conventional solid-state technique. The required ratio of ZnO (99.99% purity) and MgO (99.98% purity) was mixed with distilled water or $MnSO_4$ aqueous solution and dried at room temperature. Then, the mixtures were compacted under compressive load to form rectangle-shaped samples. These latter were sintered in air at 1100 °C for 3 h and cooled with the furnace down to room temperature. The average sizes of sintered samples were 6 × 4 × 2 mm^3.

In all samples, Mn content was 0.1 at.%. As the solubility limit of Mg in ZnO under the formation of solid solution at thermodynamic conditions was shown to be observed at $x = 0.2$ [14–17], so $x = 0.25$ was chosen to obtain reliable hexagonal-phase ZnMgO with the largest bandgap energy [17].

The X-ray diffraction (XRD), electron paramagnetic resonance (EPR), diffuse reflectance, photocurrent (PC), photoluminescence (PL) and cathodoluminescence (CL) spectra of prepared ceramics were measured at 290 K. XRD patterns were recorded using X'Pert PRO MDR X-ray diffractometer with CuK_α radiation ($\lambda = 0.15418$ nm). EPR spectra were obtained using the upgraded X-band Varian E−12 spectrometer with a sensitivity limit of about 10^{12} EPR centers. Diffuse reflectance spectra were recorded with respect to the $BaSO_4$ standard by means of a double-beam spectrometer UV-3600 UV–vis NIR (Shimadzu Company) equipped with an integrating sphere ISR-3100. Based on the Kubelka-Munk ratio, recorded spectra were converted to absorption ones using standard software. The PC spectra were registered using a home-made setup with sensitivity down to 1 × 10^{-11} A. Photoluminescence was excited using a 337-nm N_2 laser source. The CL measurements were carried out on a Leica 440 SEM at an accelerating voltage of 20 kV. The CL spectra were recorded in 200–1000 nm spectral range by using a Hamamatsu PMA-11 CCD camera and corrected for the response of the collection system.

For diffuse reflectance, PC, PL and CL registration, the samples were cut transversally and these characteristics were recorded from the cleaved surface. For PC measurements, ohmic indium electrodes were melted on the cleaved surface and direct electric field of 10 V/cm was applied.

3. Results and discussion

XRD patterns of $Zn_{0.75}Mg_{0.25}$O:Mn as well as ZnO and MgO ceramics are shown in Fig. 1. These patterns demonstrate that both ZnO-based hexagonal phase {(100), (002), (101) and (102) peaks} as well as MgO based cubic one {(111) and (020) peaks} are present in

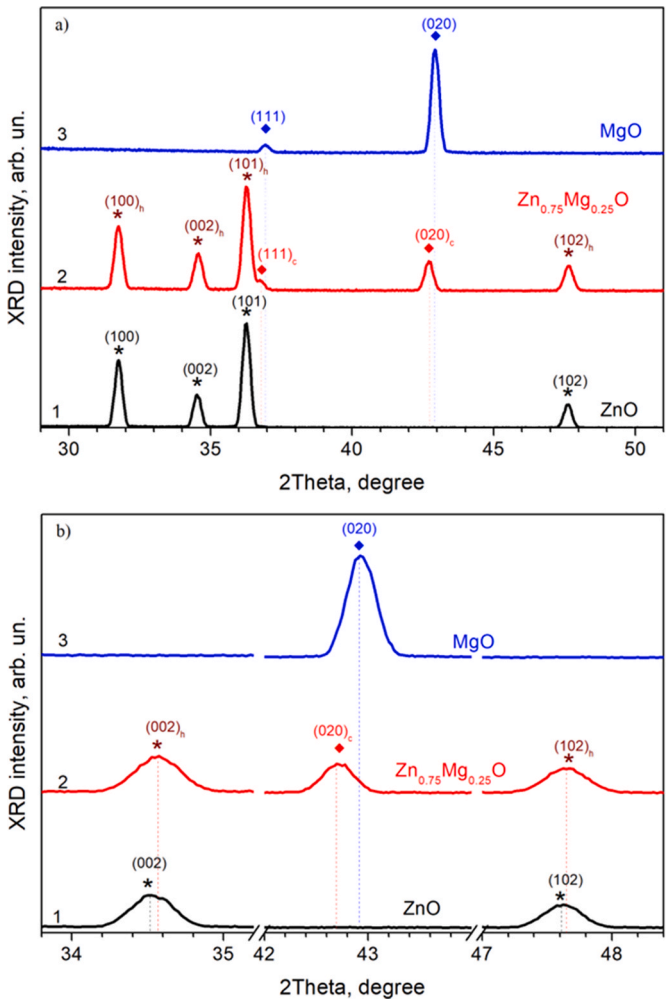

Fig. 1. a) XRD patterns of ZnO:Mn (1), $Zn_{0.75}Mg_{0.25}$O:Mn (2) and MgO:Mn (3) ceramics; b) detailed presentation of some XRD reflexes of the same ceramics.

$Zn_{0,75}Mg_{0.25}$O:Mn samples.

The shift of hexagonal phase peaks toward higher angles with respect to ZnO ones is clearly seen in Fig. 1,b. For instance, the (002) and (102) peaks shift from 3.517° to 34.752° and from 47.608° to 47.652°, respectively (Fig. 1,b, curves 1,2). At the same time, the position of the cubic (020) reflex moves to the lower angles with respect to MgO ones, i. e. from 42.917° to 42.707° (Fig. 1,b, curves 2,3). This transformation of XRD patterns indicates that both hexagonal (Zn,Mg)O and cubic (Mg,Zn)O solid solutions are formed simultaneously during the sintering process. No Mn-related phase was detected and the shift of XRD peaks due to manganese doping was not observed.

The presence of Mn-doped hexagonal and cubic phases in the obtained ceramics is confirmed by the EPR experiment. The EPR spectra of the same samples are shown in Fig. 2. The EPR spectrum of MgO:Mn (curve 1) shows the equidistant sextet from Mn_{Mg}^{2+} centers in a cubic MgO lattice. The signal from ZnO:Mn sample corresponds to the paramagnetic centers with lower-symmetrical surroundings, being characteristic for Mn_{Zn}^{2+} centers in the hexagonal ZnO lattice (curve 2), respectively.

The EPR spectrum of $Zn_{0.75}Mg_{0.25}$O:Mn ceramics (curve 3) consists of two Mn-related components. One of them is quasi-equidistant sextet being characteristic for manganese paramagnetic centers in cubic crystal fields. Its comparison with the signal from Mn_{Mg}^{2+} centers in MgO (curve 1) allows the assignment of this component to Mn_{Mg}^{2+} ions situated in the cubic MgZnO phase. Another, more complicated EPR signal, is caused by paramagnetic centers with lower-symmetrical surroundings. Its

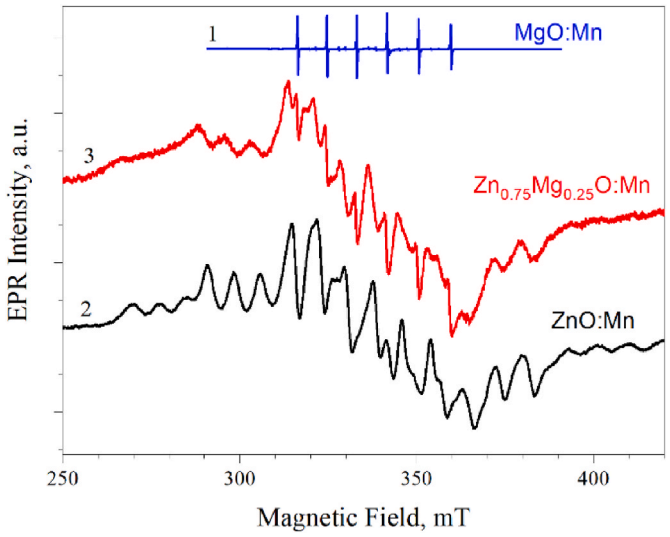

Fig. 2. EPR spectra of MgO:Mn (1), ZnO:Mn (2) and $Zn_{0.75}Mg_{0.25}O$:Mn (3) samples.

similarity with the signal of Mn_{Zn}^{2+} centers in ZnO ceramics allows the ascription of this EPR component to Mn_{Zn}^{2+} ions in the hexagonal ZnMgO phase. Thus, EPR spectra testify that the incorporation of Mn atoms in the $Zn_{0.75}Mg_{0.25}O$ host occurs both in hexagonal ZnMgO and in cubic MgZnO phases via the formation of Mn_{Zn}^{2+} and Mn_{Mg}^{2+} centers, respectively. The higher intensity of the EPR component from Mn_{Zn}^{2+} ions in the hexagonal $Zn_{0.75}Mg_{0.25}O$ phase indicates its dominant contribution to ceramic structure.

Optical absorption and PC spectra of $Zn_{0.75}Mg_{0.25}O$:Mn and ZnO:Mn ceramics are shown in Fig. 3,a and Fig. 3,b, accordingly. The absorption spectra for undoped ZnO and $Zn_{0,75}Mg_{0,25}O$ are also shown in Fig. 3a (curves 3, 4), whereas PC spectra of these samples were not obtained because of too high dark conductivity.

One can see that optical absorption and PC spectra in Mn-doped solid solution are similar to ZnO:Mn ones: side by side with excited by UV light intrinsic absorption and PC, broad unstructured extrinsic bands are observed in a visible spectral region. In $Zn_{0.75}Mg_{025}O$:Mn samples, both intrinsic and extrinsic bands are blue-shifted with respect to those in ZnO:Mn ceramics.

Band-gap value E_g for investigated samples can be estimated from the free exciton position as well as from the position of intrinsic PC maximum which coincides with that of free exciton [18]. The latter are hardly visible in absorption curves for doped ceramics, but reveal themselves distinctly in PL (Fig. 3b) and cathodoluminescence spectra shown below. Taking into account exciton binding energy in ZnO (60 meV) which has been shown to be, in fact, the same for hexagonal $Zn_{1-x}Mg_xO$ solid solution [19], one can obtain $E_{g1} = 3.32$ eV for ZnO:Mn sample and $E_{g2} = 3.65$ eV for $Zn_{0.75}Mg_{0.25}O$:Mn ceramics. So, the increase of band-gap value for $Zn_{0.75}Mg_{0.25}O$ with respect to ZnO is $\Delta E_g = 0.33$ eV.

For each sample, the onsets of Mn-related absorption and PC bands coincide and are detected at 620 nm (2.0 eV) in ZnO:Mn and at 575 nm (2.16 eV) in $Zn_{0.75}Mg_{0.25}O$ ceramics. Thus, Mn_{Zn}^{2+} energy level, E_{Mn}, resides at 2.0 eV below the *c*-band bottom for ZnO:Mn (which is in accordance with literature data [4,8,10–12]) and at 2.16 eV below the *c*-band bottom for $Zn_{0,75}Mg_{0,25}O$:Mn samples (Fig. 4a and b).

The coincidence of absorption and PC spectra onsets indicates that, in prepared $Zn_{0.75}Mg_{0.25}O$:Mn solid solution as well as in ZnO:Mn ceramics, all excited Mn_{Zn}^{2+} ion states, including the lowest one, reside inside *c*-band, which implies the absence of Mn-related emission [8]. This conclusion is confirmed by the analysis of obtained PL and CL spectra (Figs. 5 and 6, respectively).

Recorded under N_2 laser excitation (337 nm) PL spectra of undoped

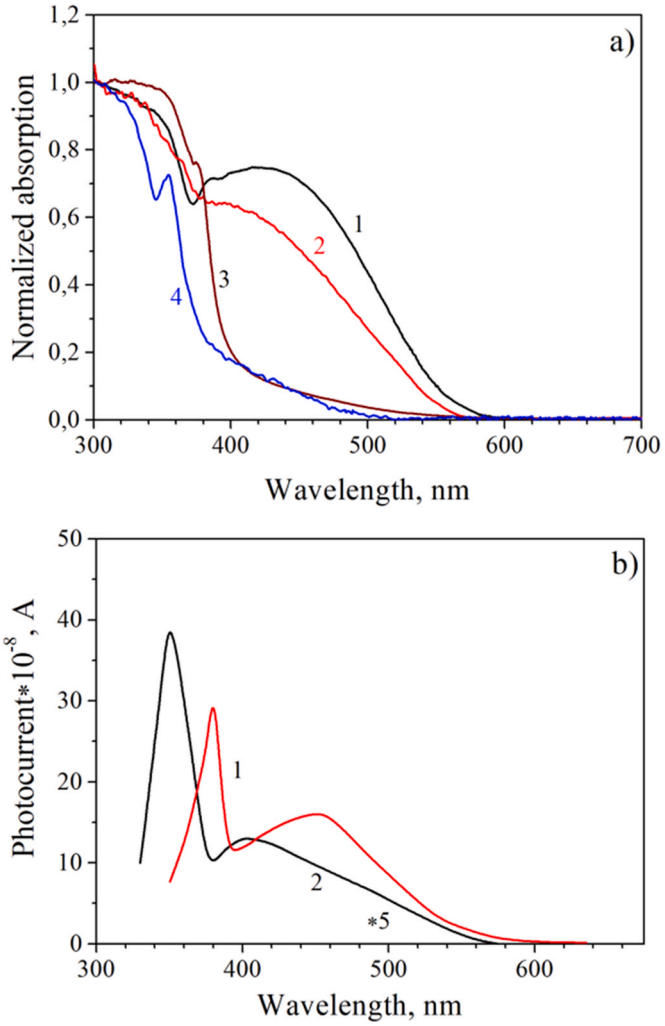

Fig. 3. Normalized optical absorption (a) and photoconductivity (b) spectra of ZnO:Mn (1), $Zn_{0.75}Mg_{0.25}O$:Mn (2), ZnO (3) and $Zn_{0.75}Mg_{0.25}O$ (4).

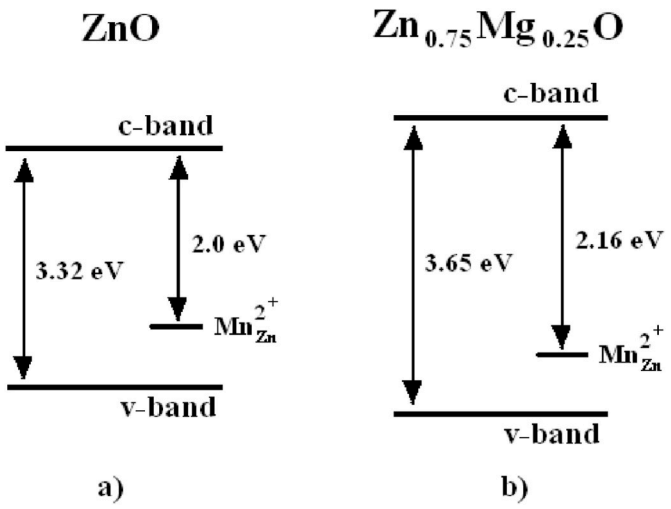

Fig. 4. Energy level diagram for Mn_{Zn}^{2+} centers in ZnO:Mn (a) and hexagonal $Zn_{0,75}Mg_{0,25}O$:Mn (b) ceramics.

$Zn_{0.75}Mg_{0.25}O$ ceramics demonstrate bright emission in the 400–650 nm spectral range (Fig. 5, curve 1) which, as previous studies have shown, consists of some overlapping bands related to native defects and residual

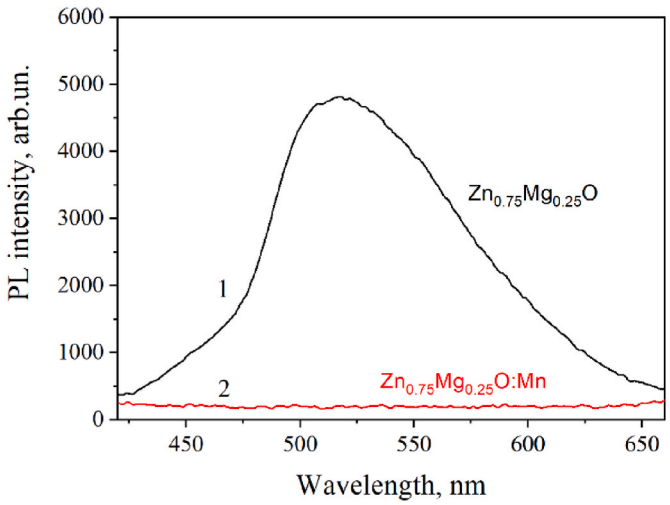

Fig. 5. PL spectra of undoped (1) and Mn-doped (2) $Zn_{0.75}Mg_{0.25}O$ ceramics ($\lambda_{exc.} = 337$ nm).

Cu impurity [20]. This defect-related emission is quenched by Mn doping and no new PL band appears (Fig. 5, curve 2) as well as it takes place in ZnO:Mn [4–8].

CL spectra of ZnO:Mn, $Zn_{0.75}Mg_{0.25}O$:Mn and MgO:Mn samples are shown in Fig. 6. High intensity of excitation by electron beam enables to observe the emission from ZnO:Mn as well as from both hexagonal and cubic phases in solid solution which is imperceptible under laser excitation, and defect-related CL for MgO:Mn sample is also recorded. In CL spectra of ZnO:Mn samples exciton PL band at 380 nm and characteristic for undoped ZnO emission in the visible spectral region related to native defects and residual Cu impurity [20] are present (Fig. 6,a).

The CL spectra of $Zn_{0.75}Mg_{0.25}O$:Mn sample exhibit exciton emission from the hexagonal phase at 350 nm, the weak broad band in 400–650 nm spectral region and relatively intense red one peaked at 750 nm (Fig. 6,b). The former is obviously defect-related emission in hexagonal-phase solid solution [20] and the latter is quite similar to 750 nm band in MgO:Mn ceramics (Fig. 6,c). This red band is usually observed in MgO doped with manganese and has been shown to result from radiative transitions in Mn^{2+}_{Mg} centers [21]. So, one can believe that the emission band at 750 nm in solid solution originates from Mn-related centers in the cubic phase (Fig. 2, curve 3). Any emission band that could be related to Mn^{2+}_{Zn} centers was observed in neither PL nor CL spectra of the prepared solid solution. This means that the distance of the first excited manganese level from the ground one in hexagonal ZnMgO exceeds 2.16 eV, while in the cubic phase of solid solution and MgO this distance (splitting manganese levels in the crystal field) is less and does not change noticeably due to MgO doping with Zn. So, obtained increase of E_g in hexagonal zinc-magnesium solid solution prepared under thermodynamic conditions is insufficient to put down the lowest Mn^{2+}_{Zn} exited state inside the band gap.

Although there are many reports on Mn intra-ionic luminescence in different hosts, such as ZnS nanoparticles [22] or CdS [23], Mn-related luminescence is scarcely observed in oxides [24]. In some cases, such as for ZnO [25], In_2O_3 [26] or SnO_2 [27], Mn doping is involved in the reduction or promotion of oxygen defect centers or excitonic emission depending on the Mn concentration.

It should be noted that nonequilibrium processes, such as PLD or MBE technique, enable the magnesium solubility limit to be exceeded and hexagonal-phase ZnMgO alloy with $E_g \geq 4.0$ eV to be prepared [28–31]. Perhaps, such an increase of E_g would ensure the disposition of the lowest Mn^{2+}_{Zn} excited state in the band gap, which should result in the appearance of Mn-related emission. However, to our best knowledge, the influence of Mn doping on the characteristics of these films has not been reported. So, further investigation of ZnMgO:Mn alloys ought to be

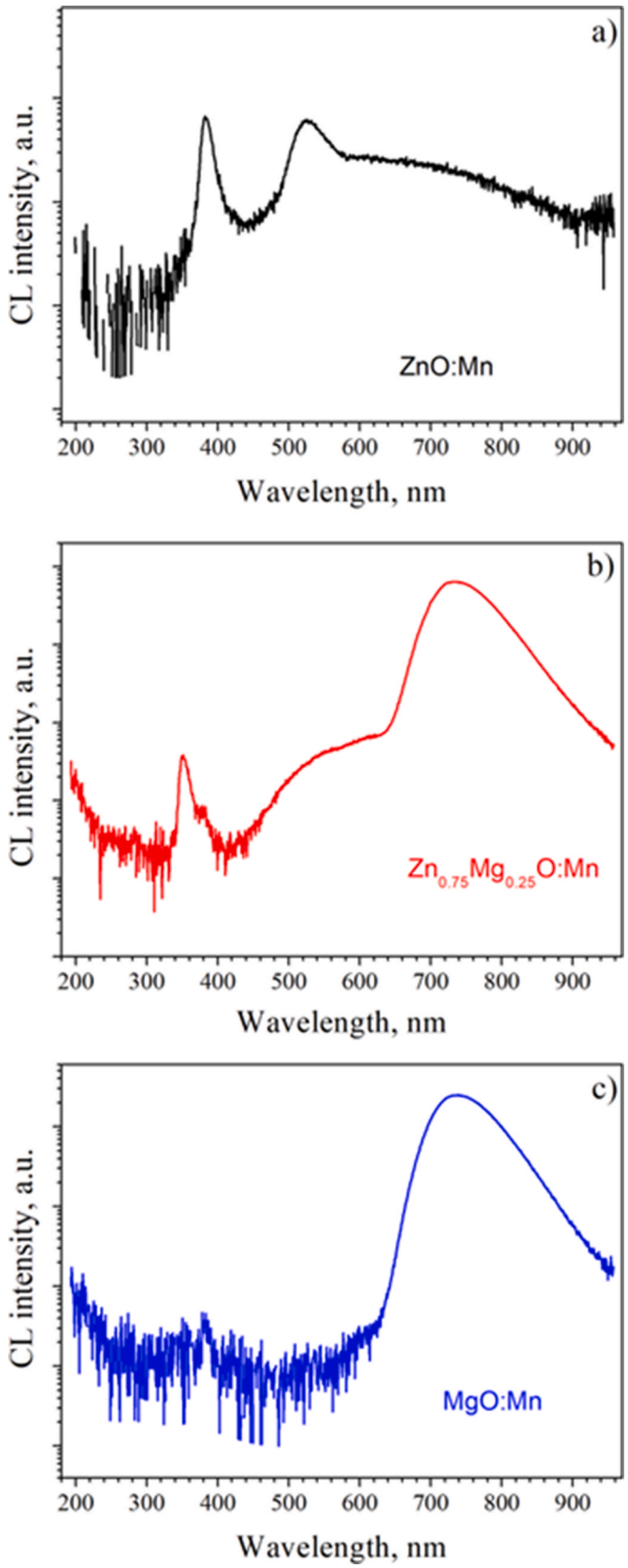

Fig. 6. CL spectra of ZnO:Mn (a), $Zn_{0.75}Mg_{0.25}O$:Mn (b) and MgO:Mn (c) ceramics.

performed.

4. Conclusion

$Zn_{0.75}Mg_{0.25}O$:Mn samples with manganese content of 0.1 at% were prepared under thermodynamic conditions by sintering ZnO and MgO powders for 3 h in air at 1100 °C. Zinc-magnesium oxide alloy consisting of a dominant hexagonal phase with band gap $E_g = 3.65$ eV and some cubic phase was obtained. Hexagonal phase absorption and photocurrent (PC) spectra exhibit broad unstructured bands in the visible spectral region. These bands originate from the photoionization of Mn_{Zn}^{2+} ions and demonstrate the same onset at 575 nm (2.16 eV) which is blue-shifted with respect to ZnO:Mn one at 620 nm (2.0 eV). Thus, the Mn_{Zn} energy level in the prepared hexagonal-phase alloy is settled at 2.16 eV below the *c*-band bottom. The coincidence of absorption and PC spectra onsets indicates that excited states of Mn_{Zn}^{2+} ions, including the lowest one, reside in the *c*-band, which implies the absence of the emission caused by $^4T_1 \rightarrow {}^6A_1$ transitions in Mn_{Zn}^{2+} ions. This conclusion is confirmed by the analysis of photo- and cathodoluminescence spectra observed in obtained ceramics. It is assumed that preparation of ZnMgO:Mn samples by nonequilibrium techniques, which enable the production of hexagonal-phase solid solution with $E_g \geq 4$ eV, could put down the lowest Mn_{Zn}^{2+} ion excited state to band gap and should result in the appearance of Mn-related emission.

Compliance with ethical standards

The authors declare that they have no potential conflicts of interest. Human participants and animals were not involved in this research.

CRediT authorship contribution statement

I. Markevich: Conceptualization, Resources, Investigation, Writing – original draft, Writing – review & editing. **N. Korsunska:** Validation, Writing – review & editing. **T. Stara:** Investigation, Formal analysis, Visualization, Writing – review & editing. **Yu Polishchuk:** Investigation, Formal analysis, Writing - review & editing. **I. Vorona:** Investigation, Formal analysis, Data curation, Writing - review & editing. **K. Kozoriz:** Investigation. **S. Ponomaryov:** Investigation, Formal analysis, Writing – review & editing. **O. Melnichuk:** Investigation, Formal analysis, Resources, Software, Funding acquisition, Writing - review & editing. **L. Melnichuk:** Investigation, Formal analysis, Writing – review & editing. **A. Cremades:** Investigation, Resources, Writing – review & editing, Funding acquisition. **L. Khomenkova:** Investigation, Formal analysis, Resources, Visualization, Funding acquisition, Writing - review & editing.

Declaration of competing interest

The authors declare that they have no known competing financial interests or personal relationships that could have appeared to influence the work reported in this paper.

Data availability

All data generated or analyzed during this study are included in this published article

Acknowledgments

This work was supported by the National Academy of Sciences of Ukraine as well as by the National Research Foundation of Ukraine from the state budget, project 2020.02/0380 «Structure transformation and non-equilibrium electron processes in wide bandgap metal oxides and their solid solutions». A. Cremades thanks the support of the project «Light-matter interaction in nano-membranes of wide bandgap metal oxides for self-powered devices» (WIDEMOX) (PID2021-122562NB-I00 Spanish Ministry for Science and Innovation).

References

[1] H.-E. Gumlich, Electro and photoluminescence properties of Mn^{2+} in ZnS and ZnCdS, J. Lumin. 23 (1981) 73–99, https://doi.org/10.1016/0022-2313(81)90191-5.
[2] J.F. Suyver, S.F. Wuister, J.J. Kelly, A. Meijerink, Luminescence of nanocrystalline ZnSe:Mn^{2+}, Phys. Chem. Chem. Phys. 2 (2000) 5445–5448, https://doi.org/10.1039/B006950G.
[3] M.A. White, A.L. Weaver, R. Belaulac, D.R. Gamelin, Electrochemically controlled Auger quenching of Mn photoluminescence in doped semiconductor nanocrystals, J. Am. Chem. Soc. 5 (2011) 4158–4168, https://doi.org/10.1021/nn200889q.
[4] M. Godlewsky, A. Wojcik-Glodowska, E. Guziewicz, S. Yatsunenko, A. Zakrzewski, Y. Dumont, E. Chikoidze, M.R. Phillips, Optical properties of manganese doped wide bandgap ZnS and ZnO, Opt. Mater. 31 (2009) 1768–1771, https://doi.org/10.1016/j.optmat.2008.12.031.
[5] M. Liu, A.H. Kitai, P. Mascher, Point defects and luminescence centers in zinc oxide and zinc oxide doped with manganese, J. Lumin. 54 (1992) 35–42, https://doi.org/10.1016/0022-2313(92)90047-D.
[6] T.R. Stara, I.V. Markevich, Influence of manganese doping on ZnO defect-related emission, Semicond. Phys. Quant. Electron. Optoelectron. 20 (2017) 137–141, https://doi.org/10.15407/spqeo20.01.137.
[7] R. Beaulac, P.L. Archer, D.R. Gamelin, Luminescence in colloidal Mn^{2+}-doped semiconductor nanocrystals, J. Solid State Chem. 181 (2008) 1582–1589, https://doi.org/10.1016/j.jssc.2008.05.001.
[8] C.A. Johnson, K.R. Kittilswtved, T.C. Kaspar, T.C. Droubay, S.A. Chambers, J. M. Salley, D.R. Gamelin, Mid-gap electronic states in $Zn_{1-x}Mn_xO$, Phys. Rev. B 82 (2010), 115202, https://doi.org/10.1103/PhysRevB.82.115202.
[9] E. Chicoidze, H.J. Bardeleben, J. Dumont, P. Galtier, J.L. Cantin, Magnetic interaction in $Zn_{1-x}Mn_xO$ studies by electron paramagnetic resaonance spectroscopy, J. Appl. Phys. 97 (2005) 10D316, https://doi.org/10.1063/1.1850372.
[10] A. Ciechan, H. Przybulinska, P. Boguslawski, A. Suchachi, A. Jekochot, A. Myciewski, P. Skupinski, K. Grasza, Metastability of Mn^{3+} in ZnO driven by strong d(Mn) intrashell Coulomb repulsion: experiment and theory, Phys. Rev. B 94 (2016), 165143, https://doi.org/10.1103/PhysRevB.94.165143.
[11] A. Tiwari, C. Jin, A. Kvit, D. Kumar, J.F. Muth, J. Narayan, Structural, optical, and magnetic properties of diluted magnetic semiconducting $Zn_{1-x}Mn_xO$ films, Solid State Commun. 121 (6–7) (2002) 371–374, https://doi.org/10.1016/S0038-1098(01)00464-1.
[12] S.J. Gilliand, J.A. Sans, J.F. Sancher-Royo, G. Almonacid, A. Segura, Charge-transfer absorption band in $Zn_{1-x}M_x$ (M: Co, Mn) investigated by means of photoconductivity, Ga doping and optical measurements under pressure, Appl. Phys. Lett. 96 (2010), 241902, https://doi.org/10.1063/1.3454243.
[13] R.N. Bhargava, V. Chhabra, T. Som, A. Ekimov, N. Taskar, Quantum confined atoms of doped ZnO nanocrystals, Phys. Status Solidi B 229 (2002) 897–901, https://doi.org/10.1002/1521-3951(200201)229:2<897::AID-PSSB897>3.0.CO;2-C.
[14] A. Singh, A. Vij, D. Kumar, P.K. Khanna, M. Kumar, S. Gautam, K.H. Chac, Investigation of phase segregation in sol-gel derived ZnMgO thin films, Semicond. Sci. Technol. 28 (2013), 025004, https://doi.org/10.1088/0268-1242/28/2/025004.
[15] Z.J. Othman, S. Ayed, A. Matoussi, H. Khemarkhem, Optical and Raman studies of $Zn_{1-x}Mg_xO$ ceramics pellets, Vib. Spectrosc. 85 (2016) 208–214, https://doi.org/10.1016/j.vibspec.2016.05.001.
[16] X. Wang, K. Saito, T. Tanaka, M. Nishio, T. Nagaoka, M. Arita, Q. Guo, Energy band bowing parameter in MgZnO alloys, Appl. Phys. Lett. 107 (2015), 022111, https://doi.org/10.1063/1.4926980.
[17] I.V. Markevich, T.R. Stara, A.V. Kuchuk, YuO. Polishchuk, V.P. Kladko, Formation of MgZnO alloy under thermodynamic conditions, Physica B: Condens. Matter 453 (2014) 123–126, https://doi.org/10.1016/j.physb.2014.05.012.
[18] L.V. Borkovska, B.M. Bulakh, V.I. Kushnirenko, I.V. Markevich, Role of excitons in the excitation of deep-level emission in ZnO crystals, Phys. Status Solidi C 7 (2010) 1605–1608, https://doi.org/10.1002/pssc.200983231.
[19] A.K. Sharma, J. Narayan, J.F. Muth, C.W. Teng, C. Jin, A. Kvit, R.M. Kolbas, O. W. Holland, Optical and structural properties of epitaxial $Mg_xZn_{1-x}O$ alloys, Appl. Phys. Lett. 75 (1999) 3327–3329, https://doi.org/10.1063/1.125340.
[20] I.V. Markevich, T.R. Stara, V.O. Bondarenko, Influence of Mg content on defect-related luminescence of undoped and doped MgZnO ceramics, Semicond. Phys. Quant. Electron. Optoelectron. 18 (2015) 344–348, https://doi.org/10.15407/spqeo18.03.344.
[21] T. Kato, G. Okada, T. Yanagide, Optical, scintillation and dosimeter properties of MgO transparent ceramics doped with Mn^{2+}, J. Ceram. Soc. Jpn. 124 (2016) 559–563, https://doi.org/10.2109/jcersj2.15229.
[22] A. Datta, S. Biswas, S. Kar, S. Chaudhuri, Multicolor luminescence from transition metal ion (Mn^{2+} and Cu^{2+}) doped ZnS nanoparticles, J. Nanosci. Nanotechnol. 7 (2007) 3670–3676, https://doi.org/10.1166/jnn.2007.810.
[23] Y. Kanemitsu, H. Matsubara, C.W. White, Optical properties of Mn-doped CdS nanocrystals fabricated by sequential ion implantation, Appl. Phys. Lett. 81 (2002) 535–537, https://doi.org/10.1063/1.1494468.
[24] Y.S. Wang, P.J. Thomas, P.J. O'Brien, Optical properties of ZnO nanocrystals doped with Cd, Mg, Mn, and Fe ions, J. Phys. Chem. B 110 (2006) 21412–21415, https://doi.org/10.1021/jp0654415.

[25] D. Shuang, X.X. Zhu, J.B. Wang, Z.L. Zhong, G.J. Huang, C. He, The influence of Mn content on luminescence properties in Mn-doped ZnO films deposited by ultrasonic spray assisted chemical vapor deposition, Appl. Surf. Sci. 257 (2011) 6085–6088, https://doi.org/10.1016/j.apsusc.2011.02.001.

[26] D. Maestre, I. Martinez de Velasco, A. Cremades, M. Amati, J. Piqueras, Micro- and nanopyramids of manganese-doped indium oxide, J. Phys. Chem. C 114 (2010) 11748–11752, https://doi.org/10.1021/jp103670b.

[27] M. Herrera, D. Maestre, A. Cremades, J. Piqueras, Growth and characterization of Mn doped SnO_2 nanowires, nanobelts, and microplates, J. Phys. Chem. C 117 (2013) 8997–9003, https://doi.org/10.1021/jp4007894.

[28] W. Yang, R.D. Vispute, S.W. Choopun, R.P. Sharma, T. Venkatesan, H. Shen, Ultraviolel photoconductor detector based on epitaxial $Mn_{0.34}Zn_{0.66}O$ thin films, Appl. Phys. Lett. 78 (2001) 2787–2789, https://doi.org/10.1063/1.1368378.

[29] A. Ohtomo, M. Kawasaki, T. Koida, K. Masubuchi, H. Koonuma, Y. Sakurai, Y. Yoshida, T. Yasuda, Y. Segawa, $Mg_xZn_{1-x}O$ as a II–VI widegap semiconductor alloy, Appl. Phys. Lett. 72 (1998) 2466–2468, https://doi.org/10.1063/1.121384.

[30] Y. Kozuka, J. Falson, Y. Segawa, T. Makino, A. Tsukazaki, M. Kawasaki, Precise calibration of Mg concentration in $Mg_xZn_{1-x}O$ thin films grown on ZnO substrates, J. Appl. Phys. 112 (2012), 043515, https://doi.org/10.1063/1.4748306.

[31] A.V. Sharma, J. Narayan, J.F. Muth, C.W. Teng, C. Lin, A. Kvit, R.M. Kolbas, O. W. Holland, Optical and structural properties of epitaxial $Mg_xZn_{1-x}O$ alloy, Appl. Phys. Lett. 75 (1999) 3327–3329, https://doi.org/10.1063/1.125340.